ISSN 0915-633X

NATIONAL INSTITUTE FOR FUSION SCIENCE

Screening Constants for Plasma

S. Kawata, S. Kato and S. Kiyokawa

(Received – Mar. 4, 1993)

NIFS-235

June 1993

RESEARCH REPORT
NIFS Series

NAGOYA, JAPAN

Screening Constants for Plasma

Shigeo Kawata, Shigeru Kato and †Syuji Kiyokawa

Department of Electrical Engineering,

Nagaoka University of Technology, Nagaoka 940-21

†*Department of Physics,*

Nara Women's University, Nara 630

Abstract

We present the improved screening constants, with which the atomic energy levels for the finite temperature materials are obtained by the screened-Hydrogen model. The improved screening constants are obtained for each of 34 materials. Each screening constants has the temperature dependence in order to realize the better reproducibility of the Hartree-Fock-Slater (HFS) energy levels. The improved screening constants provide the better results compared with More's screening constants: the improvement from the results by More's screening constants is about 40% for $n = 1$ and about 20% for $n = 2$, in average over 34 materials. Here n is the principal quantum number.

KEYWORDS: screening constants, screened-Hydrogen model, Hartree-Fock-Slater, average ion model

1. Introduction

The Hartree-Fock-Slater(HFS) model[1] is used widely in order to obtain the atomic energy levels for the finite temperature materials. However the HFS computation needs a long CPU time. On the other hand, the screening constants are used in the screened-Hydrogen energy level equation[2-6], which is solved faster numerically. The differences between the HFS energy levels and those by using More's screening constants[5,6] are about several tens eV to a few keV for $n = 1$ and 2 depending on the material and the material state, that is the density and temperature. Here n is the principal quantum number. Our aim in this paper is to reduce the gap between the two models by improving the More's screening constants. Recently R.Marchand et. al.[7] presented the analytical expressions for the screening constants, and P.Blottiau et. al[8]. improved More's screening constants by fitting the exsisting data in the non-relativistic case. In this paper we presented the screening constants for each materials in order to improve the screening constants more. When we improved the screening constants for each of 34 materials as shown in Table 3, we introduced the electron temperature dependency of the screening constants for the specified material in order to realize the better reproducibility of the HFS atomic energy levels.

2. Computational Method

The relativistic energy level employed in the screened-Hydrogen model is as follows:

$$\epsilon_n = -511 \times 10^3 \left[\left\{ 1 + \frac{\alpha^2 q_n^2}{\left(n - |\bar{k}| + \sqrt{\bar{k}^2 - \alpha^2 q_n^2} \right)^2} \right\}^{-1/2} - 1 \right] - \Delta E \qquad [eV] \,, \qquad (1)$$

where α is the fine-structure constant, q_n the effective nuclear charge, ΔE the potential lowering energy[4,5]($\Delta E = ze^2/\lambda$, where $z = z_{nc} - \sum_{n=1}^{nmax} P_n$, $\lambda = max(\lambda_D, r_s)$, λ_D is the Debye length, $r_s = (3/4\pi N)^{\frac{1}{3}}$ and N is the ion number density), and $\bar{k}$ the quantum number k averaged over the electron population:

$$\bar{k} = \frac{\sum_k P_{m,k} k}{\sum_k P_{m,k}} \quad . \qquad (2)$$

In the paper we use the following expression for the effective nuclear charge

$$q_n = z_{nc} - \sum_{m=1}^{nmax} \sigma_{nm} P_m \quad , \qquad (3)$$

where z_{nc} is the nuclear charge. Here $nmax$ is the upper limit of principal quantum number and is 10. The population P_m is the total number of electrons at the principal quantum number m: $P_m = \sum_k P_{m,k}$. The screening constant σ_{nm} represents the ratio with which the electrons at n are screened by the electrons at m. Table 1 shows More's screening constants σ_{nm}^{M} [5,6].

The difference between σ_{nm}^{M} and the improved screening constant is denoted by $\Delta\sigma_{nm}$. In the improvement procedure we compute $\Delta\sigma_{nm}$ for each material.

$$\sigma_{nm} = \sigma_{nm}^{M} + \Delta\sigma_{nm} \quad . \qquad (4)$$

The difference X between the effective charge by eq.(3) and the HFS one is

$$X = \left[z_{nc} - \sum_{m=1}^{nmax} \sigma_{nm} P_m^{HFS} \right] - q_n^{HFS} \quad . \tag{5}$$

Here q_n^{HFS} is obtained from eq.(1) by using ϵ_n^{HFS} instead of ϵ_n. Here ϵ_n^{HFS} and P_m^{HFS} are obtained by the HFS computation[1)]. The computations for Relativistic Hartree-Fock-Slater model with the central-field approximation and the Fermi Statistics were performed in order to obtain P_m^{HFS} and ϵ_n^{HFS}; we employed the computational method presented by Rozsnyai[1]. In order to obtain $\Delta\sigma_{nm}$, we employ the least square method; the total of the differences between the right and left hand sides in eq.(6) for the specified plasma density and temperature are minimized.

$$\begin{aligned} S_0 &= \sum_i \left[X^i \right]^2 \\ &= \sum_i \left[z_{nc} - \sum_{m=1}^{nmax} \sigma_{nm}^M P_m^i - q_n^i - \sum_{m=1}^{nmax} \Delta\sigma_{nm} P_m^i \right]^2 \quad , \end{aligned} \tag{6}$$

$$\begin{aligned} \frac{dS_0}{d\Delta\sigma_{nj}} &= -2 \sum_i P_j^i \left[z_{nc} - \sum_{m=1}^{nmax} \sigma_{nm}^M P_m^i - q_n^i - \sum_{m=1}^{nmax} \Delta\sigma_{nm} P_m^i \right] \\ &= -2 \sum_i P_j^i \left[Y^i - \sum_{m=1}^{nmax} \Delta\sigma_{nm} P_m^i \right] = 0 \quad , \quad (j = 1 \sim 10) \quad , \end{aligned} \tag{7}$$

where

$$Y^i = z_{nc} - \sum_{m=1}^{nmax} \sigma_{nm}^M P_m^i - q_n^i \quad .$$

Here the superscript i is used to distinguish the plasma state in the specified material. The

set of linear equations obtained is as follows:

$$\begin{pmatrix} [P_1^2] & [P_1P_2] & [P_1P_3] & \dots & [P_1P_{10}] \\ [P_1P_2] & [P_2^2] & [P_2P_3] & \dots & [P_2P_{10}] \\ \vdots & \vdots & \vdots & \ddots & \vdots \\ [P_1P_{10}] & [P_2P_{10}] & [P_3P_{10}] & \dots & [P_{10}^2] \end{pmatrix} \begin{pmatrix} \Delta\sigma_{n1} \\ \Delta\sigma_{n2} \\ \vdots \\ \Delta\sigma_{n10} \end{pmatrix} = \begin{pmatrix} [P_1Y] \\ [P_2Y] \\ \vdots \\ [P_{10}Y] \end{pmatrix} \tag{8}$$

where

$$[P_1^2] = \sum_i P_1^{i2} \quad , \quad [P_1P_2] = \sum_i P_1^i P_2^i \quad , \quad [P_1Y] = \sum_i P_1^i Y^i \ .$$

From the physically consistent point of view, the new screening constants should be remain less than or equal 1. In order to keep this feature easily, we modified S_0 to S which is

$$S = S_0 + \sum_{m=1}^{10} A_m \Delta\sigma_{nm}^2 \quad . \tag{9}$$

Here, A_m is an adjustable constant which is chosen appropriately. The equations modified by using S are

$$\begin{pmatrix} [P_1^2]+A_1 & [P_1P_2] & [P_1P_3] & \dots & [P_1P_{10}] \\ [P_1P_2] & [P_2^2]+A_2 & [P_2P_3] & \dots & [P_2P_{10}] \\ \vdots & \vdots & \vdots & \ddots & \vdots \\ [P_1P_{10}] & [P_2P_{10}] & [P_3P_{10}] & \dots & [P_{10}^2]+A_{10} \end{pmatrix} \begin{pmatrix} \Delta\sigma_{n1} \\ \Delta\sigma_{n2} \\ \vdots \\ \Delta\sigma_{n10} \end{pmatrix} = \begin{pmatrix} [P_1Y] \\ [P_2Y] \\ \vdots \\ [P_{10}Y] \end{pmatrix} \quad . \tag{10}$$

In eqs. (10) the populations P_n and ϵ_n, which are used in the effective charge q_n and Y, are obtained by the HFS computation[1].

3. Screening constants for n=1 and 2

The values of More's screening constants approach to 1 with the increase in n. If the screening constants are allowed to be larger than 1, the HFS energy levels can be

reproduced better . However, it is unreasonable from the physycally consistent point of view. In addition, the discrepancy between the HFS and screened-Hydrogen energy levels with More's screening constants can not be disregarded for $n = 1$ and 2. For example, the differences averaged over the plasma states are about $100eV$ for Al and about $1keV$ for Pb for $n = 1$ and 2. Therefore we limited ourselves to improve σ_{nm} for $n = 1$ and 2 .

When we improved More's screen constants, we introduced the temperature dependence of σ_{nm} for the specified material in order to realize the better reproducibility of the HFS atomic energy levels. We obtained the screening constants σ_{nm}^{L} at $T \leq T_0$ and σ_{nm}^{H} at $T > T_0$. Here, T_0 is the boundary temperature and depends on the material. The improved screening constants for 34 materials are shown in Tables 2.1-2.34 for $n = 1$ and 2. The new screening constants can be used in the region of $10eV \leq T \leq 100keV$ and $\frac{1}{100} \leq$ density/solid density ≤ 100. In Figs. 1-4 we also present the atomic energy levels ϵ_n for several materials. In order to evaluate the results by the new screening constants, we introduce the improvement factor R_n:

$$R_n(\%) = \left(1 - \frac{\sum_i |\epsilon_n^{i,HFS} - \epsilon_n^{i,new}|}{\sum_i |\epsilon_n^{i,HFS} - \epsilon_n^{i,More}|}\right) \times 100 \quad (n = 1 \, or \, 2) \quad , \tag{11}$$

where the superscript i is used to distinguish the plasma state in the specified material, $\epsilon_n^{i,HFS}$ is the energy level by the HFS model, $\epsilon_n^{i,More}$ one by using More's screening constants, and $\epsilon_n^{i,new}$ one by using the improved screening constants. By using R_n, we can find the improvement ratio. When R_n approaches to 100%, it means $\epsilon_n^{i,new}$ approaches to $\epsilon_n^{i,HFS}$.

Table 3 shows R_n averaged over the plasma states for 34 materials. It shows that the improved screening constants reproduce the HFS energy levels better than More's one by 38.9% for $n = 1$ and 18.3% for n=2, in average. For the high-Z materials the improvement ratio becomes large. Equations (1)-(3) associating with the screening constants are coupled with the rate equations for the population P_m in order to obtain the self-consistent P_m.

4. Conclusions

In this paper, we presented the improved screening constants in order to reproduce the HFS atomic energy levels well for the finite temperature materials. The new screening constants were obtained for 34 materials shown in Table 2. These constants reproduce the HFS energy levels better than More's ones by about 40% for $n = 1$ and about 20% for $n = 2$.

Acknowledgements

This work was partly supported by the cooperative program of the National Institute for Fusion Science and by the Scientific Reseach Fund of the Ministry of Education, Science and Culture in Japan.

References

[1]B.F.Rozsnyai, Phys. Rev. **A5**,1137(1972).

[2]W.A.Lokke and W.H.Grasberger, Lawrence Livermore Laboratory No.UCRL-52276(1977).

[3]M.Itoh, T.Yabe and S.Kiyokawa, Phys. Rev. **A35**,233(1987).

[4]G.B.Zimmerman and R.M.More, J.Quant.Spectrosc.Radiat.Transfer **23**,517(1980).

[5]R.M.More, Lawrence Livermore Laboratory No.UCRL-84991(1981).

[6]R.M.More, J.Quant.Spectrosc.Radiat.Transfer **27**,345(1982).

[7]R.Marchand, S.Caillé and Y.T.Lee, J.Quant.Spectrosc.Radiat.Transfer **43**,149(1990).

[8]P.Blottiau and G.Damamme, J.Quant.Spectrosc.Radiat.Transfer **47**,127(1992).

Table captions

Table 1. More's screening constants employed in the screened hydrogen model.

Table 2.1-34. Improved screening constants for 34 materials in $n = 1$ and $n = 2$. We introduced the electron temperature dependency in order to realize the better reproducibility of the HFS energy levels.

Table 3. Improvement factor R of the improved screening constants by Eqs.(11). The improvement factor R is averaged over the plasma states. When R approaches to 100% , it means that the energy level by using the improved screening constants approaches the HFS one.

Table 1 : More's screening constants employed by the screened-Hydrogen model

m \ n	1	2	3	4	5	6	7	8	9	10
1	.3125	.9380	.9840	.9954	.9970	.9970	.9990	.9999	.9999	1.000
2	.2345	.6038	.9040	.9722	.9979	.9880	.9900	.9990	.9990	1.000
3	.1093	.4018	.6800	.9155	.9796	.9820	.9860	.9900	.9920	1.000
4	.0622	.2430	.5150	.7100	.9200	.9600	.9750	.9830	.9860	.990
5	.0399	.1597	.3527	.5888	.7320	.8300	.9000	.9500	.9700	.980
6	.0277	.1098	.2455	.4267	.5764	.7248	.8300	.9000	.9500	.970
7	.0204	.0808	.1811	.3184	.4592	.6098	.7374	.8300	.9000	.950
8	.0156	.0624	.1392	.2457	.3711	.5062	.6355	.7441	.8300	.900
9	.0123	.0493	.1102	.1948	.2994	.4222	.5444	.6558	.7553	.830
10	.0100	.0400	.0900	.1584	.2450	.3492	.4655	.5760	.6723	.765

Table 2.1 : Improved screening constants for H

Temperature	$_n{}^m$	1	2	3	4	5	6	7	8	9	10
$T \leq 100eV$	1	.4538	.2348	.1093	.0623	.0399	.0277	.0204	.0156	.0123	.0100
	2	.9945	.6178	.4051	.2438	.1597	.1098	.0808	.0624	.0493	.0400
$T > 100eV$	1	.4538	.2348	.1093	.0623	.0399	.0277	.0204	.0156	.0123	.0100
	2	.9945	.6178	.4051	.2438	.1597	.1098	.0808	.0624	.0493	.0400

Table 2.2 : Improved screening constants for Li

Temperature	$_n{}^m$	1	2	3	4	5	6	7	8	9	10
$T \leq 100eV$	1	.4310	.2233	.1094	.0641	.0419	.0279	.0205	.0156	.0123	.0100
	2	.9910	.6068	.4028	.2433	.1599	.1098	.0808	.0624	.0493	.0400
$T > 100eV$	1	.6188	.1039	.0981	.0665	.0419	.0289	.0213	.0156	.0123	.0100
	2	.9885	.6087	.4018	.2430	.1597	.1098	.0808	.0624	.0493	.0400

Table 2.3 : Improved screening constants for C

Temperature	$_n{}^m$	1	2	3	4	5	6	7	8	9	10
$T \leq 3eV$	1	.6372	.1215	.1215	.0622	.0399	.0277	.0204	.0156	.0123	.0100
	2	1.000	.6363	.4024	.2430	.1597	.1098	.0808	.0624	.0493	.0400
$T > 3eV$	1	.3734	.2072	.1088	.0395	.0395	.0351	.0206	.0156	.0123	.0100
	2	.8344	.8344	.3680	.2270	.1510	.1081	.0808	.0624	.0493	.0400

Table 2.4 : Improved screening constants for N

Temperature	$_n{}^m$	1	2	3	4	5	6	7	8	9	10
$T \leq 10eV$	1	.4858	.1777	.0872	.0425	.0323	.0164	.0164	.0139	.0103	.0100
	2	1.000	.6321	.4037	.2434	.1599	.1098	.0809	.0624	.0493	.0400
$T > 10eV$	1	.3896	.2541	.1014	.0791	.0451	.0286	.0178	.0137	.0100	.0100
	2	.9254	.9254	.4029	.2380	.1553	.1052	.0781	.0614	.0480	.0400

Table 2.5 : Improved screening constants for O

Temperature	$_n{}^m$	1	2	3	4	5	6	7	8	9	10
$T \leq 10eV$	1	.8319	.1250	.1250	.0659	.0402	.0277	.0204	.0156	.0123	.0100
	2	1.000	.6155	.4027	.2432	.1597	.1098	.0808	.0624	.0493	.0400
$T > 10eV$	1	.3814	.2274	.1031	.0615	.0502	.0387	.0229	.0146	.0094	.0094
	2	.8828	.7951	.4559	.2654	.1468	.1326	.0874	.0573	.0378	.0378

Table 2.6 : Improved screening constants for Ne

Temperature	$_n{}^m$	1	2	3	4	5	6	7	8	9	10
$T \leq 100eV$	1	.4001	.2099	.1097	.0427	.0185	.0090	.0090	.0069	.0065	.0056
	2	.9487	.7440	.3705	.1532	.0857	.0482	.0482	.0394	.0348	.0300
$T > 100eV$	1	.6203	.2964	.0810	.0247	.0247	.0235	.0197	.0152	.0123	.0101
	2	1.000	.6299	.4048	.2436	.1599	.1099	.0808	.0624	.0493	.0400

Table 2.7 : Improved screening constants for Na

Temperature	$_n{}^m$	1	2	3	4	5	6	7	8	9	10
$T \leq 60eV$	1	.6831	.1250	.1011	.0543	.0341	.0184	.0129	.0121	.0073	.0073
	2	1.000	.6540	.4046	.2438	.1600	.1099	.0808	.0624	.0493	.0400
$T > 60eV$	1	.4843	.2684	.0607	.0187	.0185	.0149	.0149	.0123	.0095	.0087
	2	1.000	.6380	.4049	.2434	.1598	.1098	.0808	.0624	.0493	.0400

Table 2.8 : Improved screening constants for Mg

Temperature	$_n{}^m$	1	2	3	4	5	6	7	8	9	10
$T \leq 30eV$	1	.8183	.0838	.0838	.0798	.0574	.0332	.0204	.0156	.0123	.0100
	2	1.000	.7008	.4021	.2445	.1609	.1102	.0808	.0624	.0493	.0400
$T > 30eV$	1	.3884	.2712	.0876	.0876	.0521	.0362	.0247	.0151	.0115	.0086
	2	.9252	.9252	.3931	.2393	.1579	.1081	.0793	.0614	.0484	.0394

Table 2.9 : Improved screening constants for Al

Temperature	$_n{}^m$	1	2	3	4	5	6	7	8	9	10
$T \leq 30eV$	1	.9898	.0295	.0295	.0293	.0282	.0220	.0218	.0170	.0124	.0100
	2	.9870	.6521	.3829	.2424	.1596	.1098	.0808	.0624	.0493	.0400
$T > 30eV$	1	.3824	.2611	.0681	.0645	.0630	.0487	.0450	.0366	.0227	.0100
	2	.9788	.9465	.2548	.0860	.0724	.0351	.0226	.0032	.0020	.0090

Table 2.10 : Improved screening constants for Si

Temperature	$_n{}^m$	1	2	3	4	5	6	7	8	9	10
$T \leq 30eV$	1	.9898	.0295	.0295	.0293	.0282	.0220	.0218	.0170	.0124	.0100
	2	.9870	.6521	.3829	.2424	.1596	.1098	.0808	.0624	.0493	.0400
$T > 30eV$	1	.3824	.2611	.0681	.0645	.0630	.0487	.0450	.0366	.0227	.0100
	2	.9788	.9465	.2548	.0860	.0724	.0351	.0226	.0032	.0020	.0090

Table 2.11 : Improved screening constants for P

Temperature	$_n{}^m$	1	2	3	4	5	6	7	8	9	10
$T \leq 10eV$	1	.3051	.2048	.0624	.0624	.0400	.0277	.0204	.0156	.0123	.0100
	2	.9449	.6312	.2449	.2449	.1599	.1098	.0808	.0624	.0493	.0400
$T > 10eV$	1	.3716	.2466	.0495	.0325	.0279	.0218	.0218	.0178	.0150	.0117
	2	.8380	.8380	.3086	.2064	.1419	.0984	.0780	.0621	.0492	.0402

Table 2.12 : Improved screening constants for S

Temperature	$_n{}^m$	1	2	3	4	5	6	7	8	9	10
$T \leq 30eV$	1	.3040	.2006	.0630	.0630	.0403	.0279	.0205	.0157	.0123	.0100
	2	.9369	.5992	.2492	.2492	.1626	.1109	.0814	.0627	.0495	.0401
$T > 30eV$	1	.3652	.2415	.0464	.0284	.0222	.0222	.0198	.0155	.0138	.0118
	2	.8084	.8084	.3132	.1850	.1296	.0981	.0766	.0584	.0490	.0396

Table 2.13 : Improved screening constants for Cl

Temperature	$_n{}^m$	1	2	3	4	5	6	7	8	9	10
$T \leq 10eV$	1	.3120	.2325	.0614	.0614	.0405	.0280	.0205	.0157	.0123	.0100
	2	.9733	.7451	.2437	.2437	.1626	.1108	.0810	.0625	.0493	.0400
$T > 10eV$	1	.4051	.2265	.0735	.0490	.0264	.0190	.0140	.0095	.0095	.0069
	2	.9757	.7513	.3077	.1667	.0952	.0716	.0559	.0399	.0399	.0299

Table 2.14 : Improved screening constants for Ar

Temperature	$_n{}^m$	1	2	3	4	5	6	7	8	9	10
$T \leq 100eV$	1	.3622	.2281	.0679	.0573	.0573	.0390	.0323	.0157	.0120	.0088
	2	.7459	.7392	.5093	.1486	.1413	.0960	.0655	.0422	.0321	.0321
$T > 100eV$	1	.3875	.3014	.1576	.1268	.1268	.0825	.0489	.0395	.0168	.0141
	2	.9505	.9505	.5408	.2648	.1662	.1097	.0795	.0604	.0478	.0384

Table 2.15 : Improved screening constants for K

Temperature	$_n{}^m$	1	2	3	4	5	6	7	8	9	10
$T \leq 100eV$	1	.3568	.2353	.0426	.0393	.0393	.0350	.0259	.0218	.0137	.0117
	2	.7641	.7641	.3360	.1895	.1388	.1048	.0793	.0612	.0475	.0379
$T > 100eV$	1	.3874	.3060	.0922	.0821	.0821	.0633	.0354	.0277	.0169	.0116
	2	.9547	.9547	.4106	.2436	.1595	.1091	.0800	.0616	.0487	.0395

Table 2.16 : Improved screening constants for Ca

Temperature	$_n{}^m$	1	2	3	4	5	6	7	8	9	10
$T \leq 10eV$	1	.3258	.2878	.0704	.0497	.0386	.0386	.0216	.0156	.0123	.0100
	2	1.000	.8518	.4047	.2439	.1603	.1102	.0808	.0624	.0493	.0400
$T > 10eV$	1	.4265	.2150	.0515	.0515	.0318	.0227	.0162	.0137	.0103	.0090
	2	1.000	.6888	.3817	.2393	.1568	.1080	.0791	.0616	.0485	.0396

Table 2.17 : Improved screening constants for Ti

Temperature	$_n{}^m$	1	2	3	4	5	6	7	8	9	10
$T \leq 10eV$	1	.3284	.2982	.0638	.0638	.0419	.0284	.0204	.0156	.0123	.0100
	2	1.000	.8518	.4313	.2454	.1608	.1101	.0808	.0624	.0493	.0400
$T > 10eV$	1	.4722	.2055	.0473	.0343	.0228	.0142	.0120	.0070	.0070	.0058
	2	1.000	.6613	.3943	.2425	.1598	.1094	.0805	.0620	.0489	.0397

Table 2.18 : Improved screening constants for Fe

Temperature	$_n{}^m$	1	2	3	4	5	6	7	8	9	10
$T \leq 30eV$	1	.3340	.3205	.0647	.0647	.0407	.0280	.0206	.0156	.0123	.0100
	2	1.000	.8518	.4267	.2464	.1604	.1101	.0810	.0624	.0493	.0400
$T > 30eV$	1	.3095	.2221	.1080	.0319	.0319	.0247	.0197	.0153	.0123	.0100
	2	.9363	.6039	.5246	.1267	.1267	.0963	.0769	.0602	.0483	.0392

Table 2.19 : Improved screening constants for Ni

Temperature	$_n{}^m$	1	2	3	4	5	6	7	8	9	10
$T \leq 30eV$	1	.3385	.3385	.0704	.0650	.0411	.0282	.0206	.0156	.0123	.0100
	2	1.000	.8518	.4334	.2479	.1608	.1102	.0810	.0624	.0493	.0400
$T > 30eV$	1	.3094	.2219	.1032	.0322	.0322	.0244	.0193	.0150	.0122	.0099
	2	.9364	.5976	.4856	.1251	.1251	.0933	.0741	.0582	.0478	.0385

Table 2.20 : Improved screening constants for Cu

Temperature	$_n{}^m$	1	2	3	4	5	6	7	8	9	10
$T \leq 30eV$	1	.3385	.3385	.0857	.0644	.0407	.0281	.0207	.0156	.0123	.0100
	2	1.000	.8518	.4401	.2468	.1606	.1102	.0811	.0624	.0493	.0400
$T > 30eV$	1	.3096	.2227	.0918	.0315	.0239	.0190	.0167	.0131	.0131	.0109
	2	.9347	.5902	.4449	.1394	.0979	.0743	.0647	.0505	.0505	.0415

Table 2.21 : Improved screening constants for As

Temperature	$_n{}^m$	1	2	3	4	5	6	7	8	9	10
$T \leq 30eV$	1	.3373	.3339	.0644	.0644	.0416	.0286	.0208	.0158	.0124	.0100
	2	1.000	.8518	.4432	.2506	.1624	.1112	.0813	.0627	.0494	.0400
$T > 30eV$	1	.4488	.2105	.0752	.0420	.0276	.0177	.0119	.0093	.0058	.0058
	2	1.000	.6359	.3884	.2389	.1580	.1084	.0796	.0613	.0482	.0393

Table 2.22 : Improved screening constants for Kr

Temperature	$_n{}^m$	1	2	3	4	5	6	7	8	9	10
$T \leq 100eV$	1	.3568	.2353	.0426	.0393	.0393	.0350	.0259	.0218	.0137	.0117
	2	.7641	.7641	.3360	.1895	.1388	.1048	.0793	.0612	.0475	.0379
$T > 100eV$	1	.3874	.3060	.0922	.0821	.0821	.0633	.0354	.0277	.0169	.0116
	2	.9547	.9547	.4106	.2436	.1595	.1091	.0800	.0616	.0487	.0395

Table 2.23 : Improved screening constants for Nb

Temperature	$_n{}^m$	1	2	3	4	5	6	7	8	9	10
$T \leq 100eV$	1	.3277	.2954	.0629	.0376	.0376	.0289	.0215	.0163	.0127	.0104
	2	1.000	.8518	.3153	.1723	.1543	.1143	.0848	.0648	.0506	.0413
$T > 100eV$	1	.4582	.1954	.1132	.0388	.0215	.0122	.0101	.0088	.0060	.0060
	2	1.000	.6147	.4398	.2423	.1568	.1072	.0792	.0614	.0484	.0393

Table 2.24 : Improved screening constants for Mo

Temperature	$_n{}^m$	1	2	3	4	5	6	7	8	9	10
$T \leq 30eV$	1	.3195	.2627	.0837	.0339	.0339	.0276	.0208	.0158	.0123	.0100
	2	.9789	.7673	.3756	.1380	.1380	.1100	.0827	.0632	.0493	.0400
$T > 30eV$	1	.3654	.2638	.0714	.0352	.0352	.0262	.0211	.0163	.0123	.0105
	2	1.000	.7348	.3643	.2040	.1537	.1091	.0827	.0640	.0497	.0412

Table 2.25 : Improved screening constants for Ag

Temperature	$_n{}^m$	1	2	3	4	5	6	7	8	9	10
$T \leq 30eV$	1	.3117	.2313	.1020	.0401	.0401	.0278	.0204	.0156	.0123	.0100
	2	.9439	.6275	.4548	.1611	.1611	.1102	.0811	.0625	.0494	.0400
$T > 30eV$	1	.3104	.2260	.0789	.0392	.0169	.0169	.0158	.0137	.0113	.0097
	2	.9347	.5908	.3411	.2080	.0724	.0724	.0656	.0562	.0462	.0392

Table 2.26 : Improved screening constants for Cd

Temperature	$_n{}^m$	1	2	3	4	5	6	7	8	9	10
$T \leq 100eV$	1	.3104	.2260	.0789	.0392	.0169	.0169	.0158	.0137	.0113	.0097
	2	.9347	.5908	.3411	.2080	.0724	.0724	.0656	.0562	.0462	.0392
$T > 100eV$	1	.3088	.2198	.1017	.0245	.0155	.0141	.0110	.0110	.0099	.0087
	2	.9215	.5376	.4563	.1216	.0666	.0554	.0419	.0419	.0376	.0329

Table 2.27 : Improved screening constants for Sn

Temperature	$_n{}^m$	1	2	3	4	5	6	7	8	9	10
$T \leq 30eV$	1	.3117	.2313	.1020	.0401	.0401	.0278	.0204	.0156	.0123	.0100
	2	.9439	.6275	.4548	.1611	.1611	.1102	.0811	.0625	.0494	.0400
$T > 30eV$	1	.3104	.2260	.0789	.0392	.0169	.0169	.0158	.0137	.0113	.0097
	2	.9347	.5908	.3411	.2080	.0724	.0724	.0656	.0562	.0462	.0392

Table 2.28 : Improved screening constants for Xe

Temperature	$_n{}^m$	1	2	3	4	5	6	7	8	9	10
$T \leq 30eV$	1	.3126	.2349	.1101	.0403	.0403	.0280	.0206	.0157	.0123	.0100
	2	.9484	.6456	.4957	.1620	.1620	.1115	.0817	.0628	.0495	.0401
$T > 30eV$	1	.3877	.2317	.0717	.0361	.0283	.0180	.0141	.0113	.0073	.0073
	2	.9893	.6459	.3271	.1806	.1117	.0692	.0483	.0384	.0246	.0246

Table 2.29 : Improved screening constants for Cs

Temperature	$_n{}^m$	1	2	3	4	5	6	7	8	9	10
$T \leq 100eV$	1	.3093	.2219	.0807	.0397	.0240	.0240	.0197	.0152	.0123	.0100
	2	.9315	.5777	.3426	.2027	.0959	.0959	.0791	.0615	.0492	.0398
$T > 100eV$	1	.3092	.2213	.0908	.0451	.0181	.0181	.0158	.0138	.0110	.0097
	2	.9208	.5350	.4045	.2284	.0609	.0609	.0528	.0487	.0376	.0349

Table 2.30 : Improved screening constants for Ta

Temperature	$_n{}^m$	1	2	3	4	5	6	7	8	9	10
$T \leq 100eV$	1	.3137	.2394	.1204	.0401	.0401	.0280	.0206	.0157	.0124	.0101
	2	.9527	.6625	.5337	.1624	.1624	.1119	.0820	.0631	.0498	.0403
$T > 100eV$	1	.3924	.2201	.0735	.0441	.0323	.0168	.0117	.0100	.0065	.0065
	2	.9415	.6033	.3263	.2165	.1268	.0531	.0335	.0273	.0175	.0175

Table 2.31 : Improved screening constants for Os

Temperature	$_n{}^m$	1	2	3	4	5	6	7	8	9	10
$T \leq 100eV$	1	.3150	.2445	.1318	.0347	.0347	.0279	.0209	.0159	.0125	.0102
	2	.9594	.6895	.5946	.1395	.1395	.1116	.0835	.0641	.0504	.0408
$T > 100eV$	1	.4136	.2157	.0752	.0400	.0222	.0071	.0042	.0018	.0002	.0000
	2	.9256	.6058	.3338	.1984	.0958	.0292	.0131	.0052	.0030	.0000

Table 2.32 : Improved screening constants for Au

Temperature	$_n{}^m$	1	2	3	4	5	6	7	8	9	10
$T \leq 100eV$	1	.3235	.2785	.1295	.0368	.0368	.0271	.0202	.0155	.0123	.0100
	2	.9982	.8447	.5847	.1482	.1482	.1076	.0801	.0621	.0492	.0399
$T > 100eV$	1	.4186	.2089	.0743	.0397	.0348	.0205	.0148	.0065	.0028	.0001
	2	.8393	.6003	.3298	.2017	.1484	.0774	.0536	.0232	.0081	.0001

Table 2.33 : Improved screening constants for Pb

Temperature	$_n{}^m$	1	2	3	4	5	6	7	8	9	10
$T \leq 100eV$	1	.3150	.2431	.1345	.0341	.0333	.0258	.0202	.0155	.0123	.0100
	2	.9609	.6956	.6083	.1520	.1467	.1049	.0820	.0637	.0504	.0404
$T > 100eV$	1	.3689	.2154	.0745	.0441	.0275	.0273	.0236	.0179	.0134	.0100
	2	.7349	.5850	.3344	.2259	.1152	.1159	.0965	.0715	.0502	.0297

Table 2.34 : Improved screening constants for U

Temperature	$_n{}^m$	1	2	3	4	5	6	7	8	9	10
$T \leq 100eV$	1	.3147	.2433	.1290	.0376	.0376	.0275	.0204	.0158	.0125	.0101
	2	.9602	.6925	.6014	.1486	.1486	.1092	.0811	.0638	.0507	.0408
$T > 100eV$	1	.3109	.2282	.0950	.0278	.0278	.0260	.0208	.0163	.0128	.0103
	2	.9393	.6089	.4132	.1250	.1069	.1069	.0870	.0688	.0534	.0423

Table 3 : Improvement factor R

Material	n=1	n=2
H	18.1%	0.4%
Li	14.9%	4.9%
C	42.7%	7.6%
N	38.6%	14.9%
O	52.4%	4.5%
Ne	34.5%	5.0%
Na	27.3%	8.4%
Mg	49.7%	18.9%
Al	65.4%	20.0%
Si	49.1%	12.0%
P	32.6%	12.2%
S	35.3%	5.0%
Cl	12.6%	2.8%
Ar	42.3%	14.7%
K	39.8%	17.0%
Ca	38.5%	11.3%
Ti	29.5%	17.3%
Fe	35.6%	34.2%
Ni	33.7%	30.0%
Cu	36.4%	27.0%
As	36.2%	24.8%
Kr	29.2%	19.5%
Nb	31.9%	15.3%
Ag	29.2%	10.0%
Cd	28.8%	1.3%
Sn	37.7%	27.2%
Xe	56.2%	37.3%
Cs	32.5%	12.7%
Ta	50.6%	37.6%
Os	54.3%	43.6%
Au	49.1%	43.2%
Pb	71.2%	61.7%
U	40.6%	18.2%
Average	38.9%	18.3%

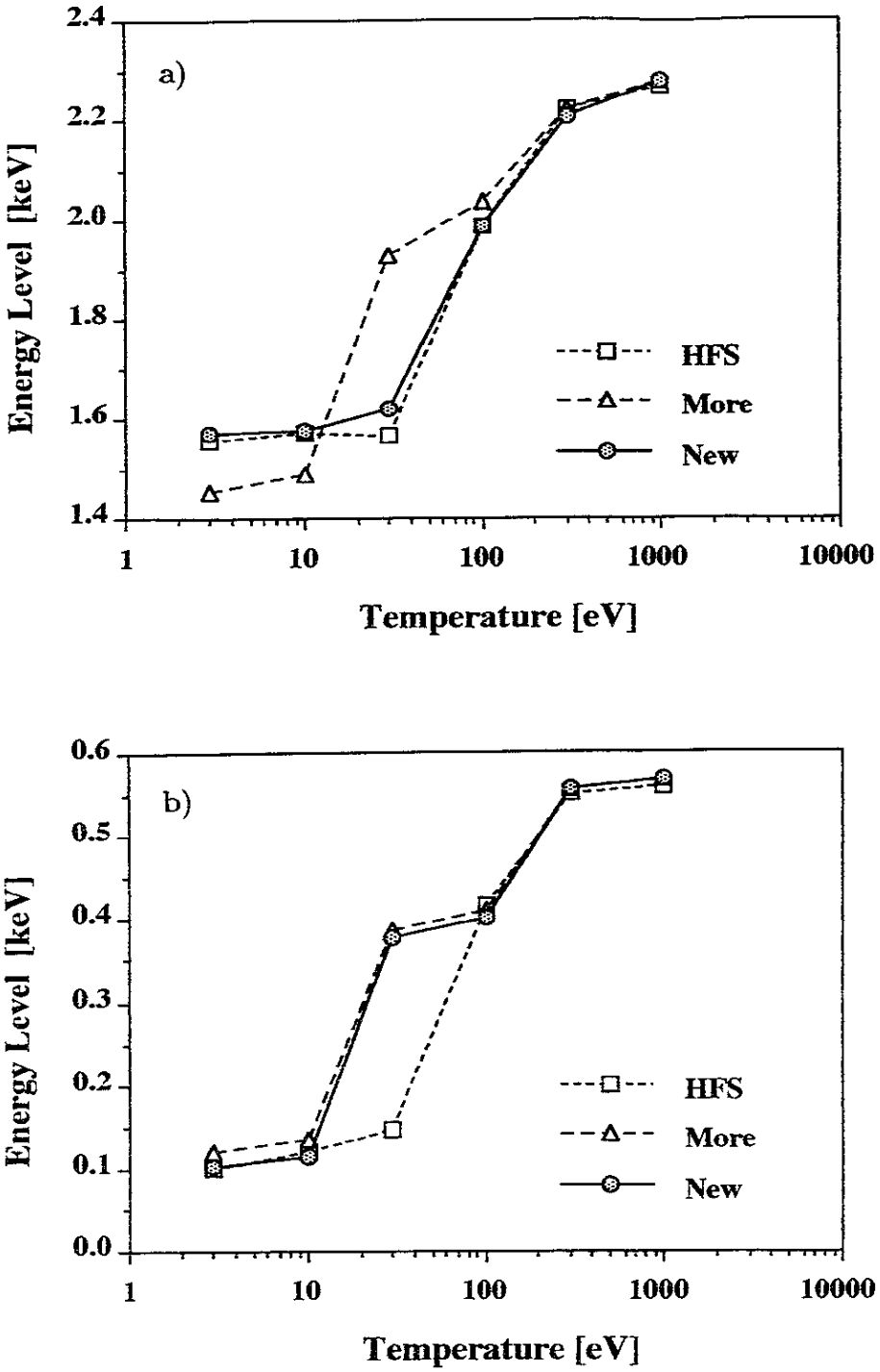

The energy levels of $n = 1$ and 2 for Al. The number densities in a) and b) are $\frac{1}{100}$ and $\frac{1}{1000}$ of solid density of Al which is $6.003937 \times 10^{22}/cc$, respectively. Square, triangular and circular symbols mean the HFS energy level, that by using More's screening constants and that by using the improved screening constants, respectively.

Fig.1

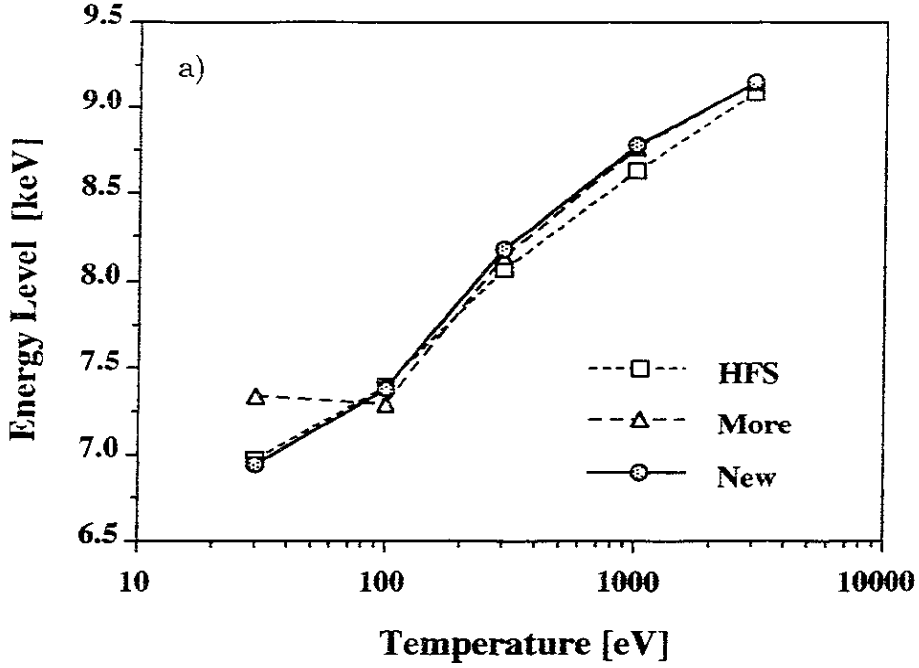

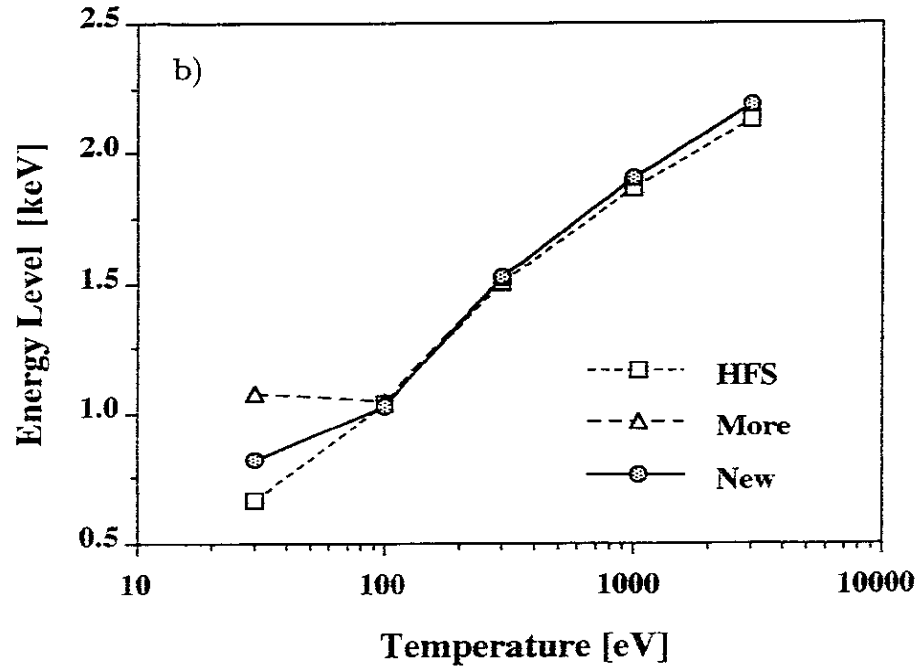

The energy levels of $n = 1$ and 2 for Fe. The number density in both a) and b) is $\frac{1}{10}$ of solid density of Fe which is $8.475656 \times 10^{22}/cc$.

Fig.2

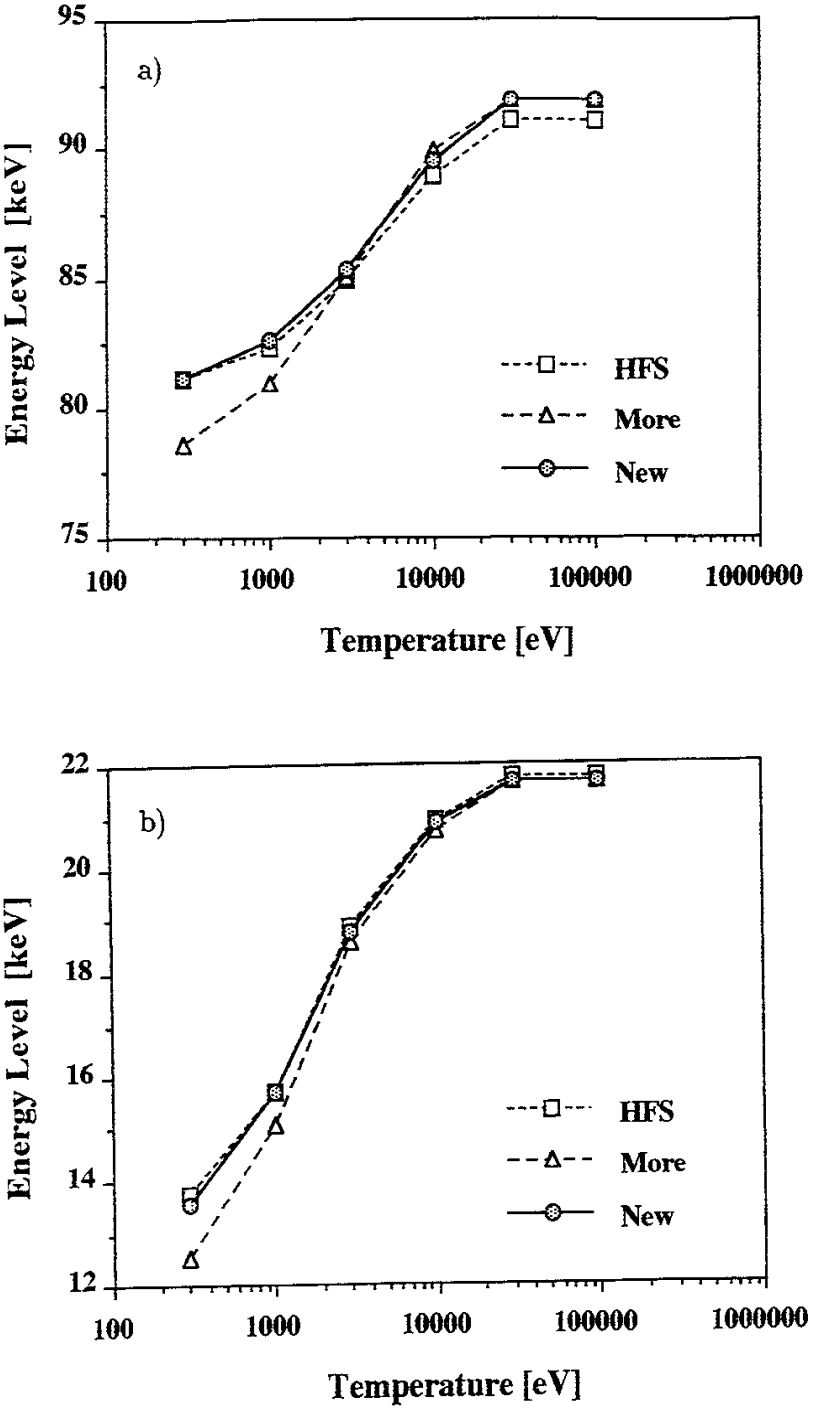

The energy levels of $n = 1$ and 2 for Au. The number densities in a) and b) are 10 times and 1 times of solid density of Au which is $5.008621 \times 10^{22}/cc$, respectively.

Fig.3

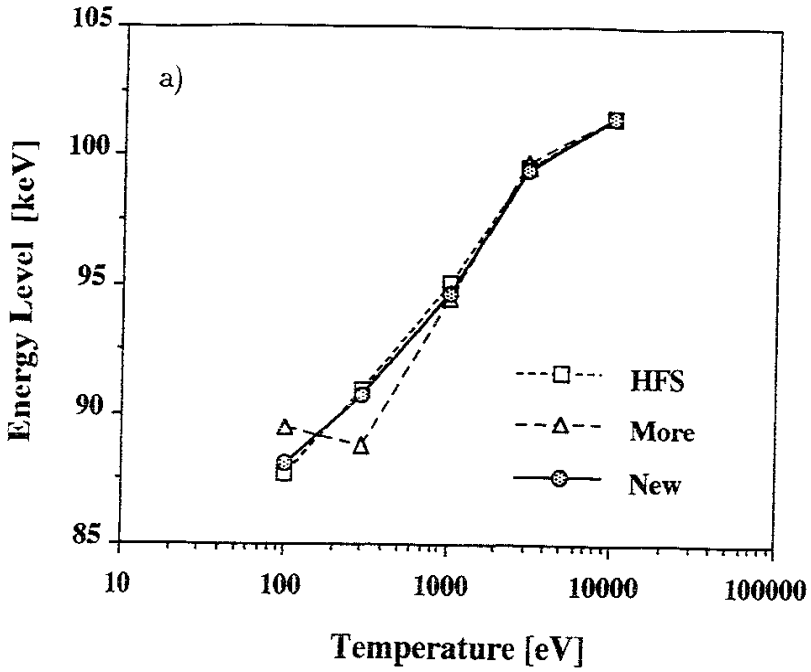

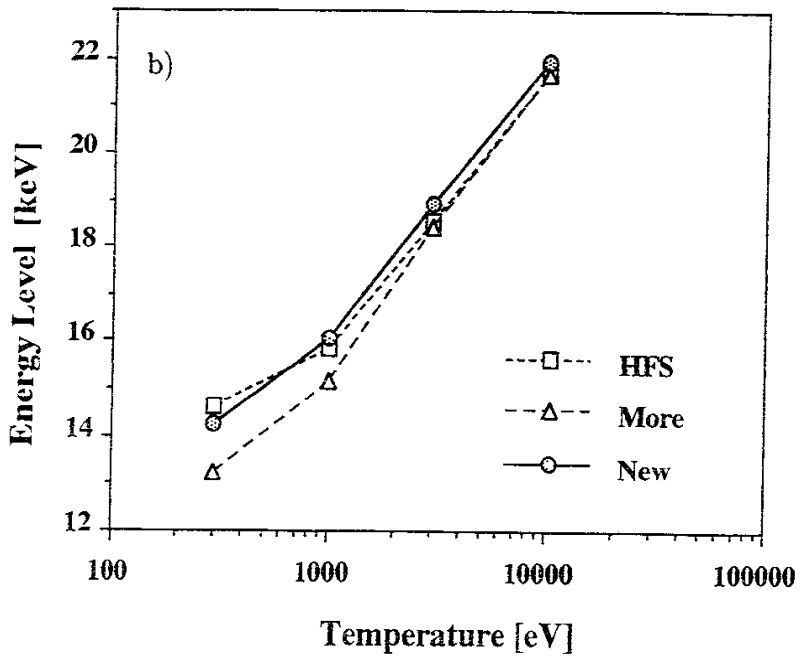

The energy levels of $n = 1$ and 2 for Pb. The number densities in a) and b) are $\frac{1}{1000}$ and 10 times of solid density of Al which is $3.295899 \times 10^{22}/cc$, respectively.

Fig.4

Recent Issues of NIFS Series

NIFS-185 H. Yamada, S. Morita, K. Ida, S. Okamura, H. Iguchi, S. Sakakibara, K. Nishimura, R. Akiyama, H. Arimoto, M. Fujiwara, K. Hanatani, S. P. Hirshman, K. Ichiguchi, H. Idei, O. Kaneko, T. Kawamoto, S. Kubo, D. K. Lee, K. Matsuoka, O, Motojima, T. Ozaki, V. D. Pustovitov, A. Sagara, H. Sanuki, T. Shoji, C. Takahashi, Y. Takeiri, Y. Takita, S. Tanahashi, J. Todoroki, K. Toi, K. Tsumori, M. Ueda and I. Yamada, *MHD and Confinement Characteristics in the High-β Regime on the CHS Low-Aspect-Ratio Heliotron / Torsatron* ; Sep. 1992

NIFS-186 S. Morita, H. Yamada, H. Iguchi, K. Adati, R. Akiyama, H. Arimoto, M. Fujiwara, Y. Hamada, K. Ida, H. Idei, O. Kaneko, K. Kawahata, T. Kawamoto, S. Kubo, R. Kumazawa, K. Matsuoka, T. Morisaki, K. Nishimura, S. Okamura, T. Ozaki, T. Seki, M. Sakurai, S, Sakakibara, A. Sagara, C. Takahashi, Y. Takeiri, H. Takenaga, Y. Takita, K. Toi, K. Tsumori, K. Uchino, M. Ueda, T. Watari, I. Yamada, *A Role of Neutral Hydrogen in CHS Plasmas with Reheat and Collapse and Comparison with JIPP T-IIU Tokamak Plasmas* ; Sep. 1992

NIFS-187 K. Ioth, S.-I. Itoh, A. Fukuyama, M. Yagi and M. Azumi, *Model of the L-Mode Confinement in Tokamaks* ; Sep. 1992

NIFS-188 K. Itoh, A. Fukuyama and S.-I. Itoh, *Beta-Limiting Phenomena in High-Aspect-Ratio Toroidal Helical Plasmas*; Oct. 1992

NIFS-189 K. Itoh, S. -I. Itoh and A. Fukuyama, *Cross Field Ion Motion at Sawtooth Crash* ; Oct. 1992

NIFS-190 N. Noda, Y. Kubota, A. Sagara, N. Ohyabu, K. Akaishi, H. Ji, O. Motojima, M. Hashiba, I. Fujita, T. Hino, T. Yamashina, T. Matsuda, T. Sogabe, T. Matsumoto, K. Kuroda, S. Yamazaki, H. Ise, J. Adachi and T. Suzuki, *Design Study on Divertor Plates of Large Helical Device (LHD)* ; Oct. 1992

NIFS-191 Y. Kondoh, Y. Hosaka and K. Ishii, *Kernel Optimum Nearly-Analytical Discretization (KOND) Algorithm Applied to Parabolic and Hyperbolic Equations* : Oct. 1992

NIFS-192 K. Itoh, M. Yagi, S.-I. Itoh, A. Fukuyama and M. Azumi, *L-Mode Confinement Model Based on Transport-MHD Theory in Tokamaks* ; Oct. 1992

NIFS-193 T. Watari, *Review of Japanese Results on Heating and Current Drive* ; Oct. 1992

NIFS-194 Y. Kondoh, *Eigenfunction for Dissipative Dynamics Operator and Attractor of Dissipative Structure* ; Oct. 1992

NIFS-195 T. Watanabe, H. Oya, K. Watanabe and T. Sato, *Comprehensive Simulation Study on Local and Global Development of Auroral Arcs and Field-Aligned Potentials* ; Oct. 1992

NIFS-196 T. Mori, K. Akaishi, Y. Kubota, O. Motojima, M. Mushiaki, Y. Funato and Y. Hanaoka, *Pumping Experiment of Water on B and LaB_6 Films with Electron Beam Evaporator* ; Oct., 1992

NIFS-197 T. Kato and K. Masai, *X-ray Spectra from Hinotori Satellite and Suprathermal Electrons* ; Oct. 1992

NIFS-198 K. Toi, S. Okamura, H. Iguchi, H. Yamada, S. Morita, S. Sakakibara, K. Ida, K. Nishimura, K. Matsuoka, R. Akiyama, H. Arimoto, M. Fujiwara, M. Hosokawa, H. Idei, O. Kaneko, S. Kubo, A. Sagara, C. Takahashi, Y. Takeiri, Y. Takita, K. Tsumori, I. Yamada and H. Zushi, *Formation of H-mode Like Transport Barrier in the CHS Heliotron / Torsatron* ; Oct. 1992

NIFS-199 M. Tanaka, *A Kinetic Simulation of Low-Frequency Electromagnetic Phenomena in Inhomogeneous Plasmas of Three-Dimensions* ; Nov. 1992

NIFS-200 K. Itoh, S.-I. Itoh, H. Sanuki and A. Fukuyama, *Roles of Electric Field on Toroidal Magnetic Confinement*, Nov. 1992

NIFS-201 G. Gnudi and T. Hatori, *Hamiltonian for the Toroidal Helical Magnetic Field Lines in the Vacuum*; Nov. 1992

NIFS-202 K. Itoh, S.-I. Itoh and A. Fukuyama, *Physics of Transport Phenomena in Magnetic Confinement Plasmas*; Dec. 1992

NIFS-203 Y. Hamada, Y. Kawasumi, H. Iguchi, A. Fujisawa, Y. Abe and M. Takahashi, *Mesh Effect in a Parallel Plate Analyzer*; Dec. 1992

NIFS-204 T. Okada and H. Tazawa, *Two-Stream Instability for a Light Ion Beam -Plasma System with External Magnetic Field;* Dec. 1992

NIFS-205 M. Osakabe, S. Itoh, Y. Gotoh, M. Sasao and J. Fujita, *A Compact Neutron Counter Telescope with Thick Radiator (Cotetra) for Fusion Experiment*; Jan. 1993

NIFS-206 T. Yabe and F. Xiao, *Tracking Sharp Interface of Two Fluids by the CIP (Cubic-Interpolated Propagation) Scheme*, Jan. 1993

NIFS-207 A. Kageyama, K. Watanabe and T. Sato, *Simulation Study of MHD*

Dynamo : Convection in a Rotating Spherical Shell; Feb. 1993

NIFS-208 M. Okamoto and S. Murakami, *Plasma Heating in Toroidal Systems*; Feb. 1993

NIFS-209 K. Masai, *Density Dependence of Line Intensities and Application to Plasma Diagnostics*; Feb. 1993

NIFS-210 K. Ohkubo, M. Hosokawa, S. Kubo, M. Sato, Y. Takita and T. Kuroda, *R&D of Transmission Lines for ECH System* ; Feb. 1993

NIFS-211 A. A. Shishkin, K. Y. Watanabe, K. Yamazaki, O. Motojima, D. L. Grekov, M. S. Smirnova and A. V. Zolotukhin, *Some Features of Particle Orbit Behavior in LHD Configurations*; Mar. 1993

NIFS-212 Y. Kondoh, Y. Hosaka and J.-L. Liang, *Demonstration for Novel Self-organization Theory by Three-Dimensional Magnetohydrodynamic Simulation*; Mar. 1993

NIFS-213 K. Itoh, H. Sanuki and S.-I. Itoh, *Thermal and Electric Oscillation Driven by Orbit Loss in Helical Systems*; Mar. 1993

NIFS-214 T. Yamagishi, *Effect of Continuous Eigenvalue Spectrum on Plasma Transport in Toroidal Systems*; Mar. 1993

NIFS-215 K. Ida, K. Itoh, S.-I.Itoh, Y. Miura, JFT-2M Group and A. Fukuyama, *Thickness of the Layer of Strong Radial Electric Field in JFT-2M H-mode Plasmas*; Apr. 1993

NIFS-216 M. Yagi, K. Itoh, S.-I. Itoh, A. Fukuyama and M. Azumi, *Analysis of Current Diffusive Ballooning Mode*; Apr. 1993

NIFS-217 J. Guasp, K. Yamazaki and O. Motojima, *Particle Orbit Analysis for LHD Helical Axis Configurations* ; Apr. 1993

NIFS-218 T. Yabe, T. Ito and M. Okazaki, *Holography Machine HORN-1 for Computer-aided Retrieve of Virtual Three-dimensional Image* ; Apr. 1993

NIFS-219 K. Itoh, S.-I. Itoh, A. Fukuyama, M. Yagi and M. Azumi, *Self-sustained Turbulence and L-Mode Confinement in Toroidal Plasmas* ; Apr. 1993

NIFS-220 T. Watari, R. Kumazawa, T. Mutoh, T. Seki, K. Nishimura and F. Shimpo, *Applications of Non-resonant RF Forces to Improvement of Tokamak Reactor Performances Part I: Application of Ponderomotive Force* ; May 1993

NIFS-221 S.-I. Itoh, K. Itoh, and A. Fukuyama, *ELMy-H mode as Limit Cycle and Transient Responses of H-modes in Tokamaks* ; May 1993

NIFS-222 H. Hojo, M. Inutake, M. Ichimura, R. Katsumata and T. Watanabe, *Interchange Stability Criteria for Anisotropic Central-Cell Plasmas in the Tandem Mirror GAMMA 10 ;* May 1993

NIFS-223 K. Itoh, S.-I. Itoh, M. Yagi, A. Fukuyama and M. Azumi, *Theory of Pseudo-Classical Confinement and Transmutation to L-Mode;* May 1993

NIFS-224 M. Tanaka, *HIDENEK: An Implicit Particle Simulation of Kinetic-MHD Phenomena in Three-Dimensional Plasmas;* May 1993

NIFS-225 H. Hojo and T. Hatori, *Bounce Resonance Heating and Transport in a Magnetic Mirror;* May 1993

NIFS-226 S.-I. Iton, K. Itoh, A. Fukuyama, M. Yagi, *Theory of Anomalous Transport in H-Mode Plasmas;* May 1993

NIFS-227 T. Yamagishi, *Anomalous Cross Field Flux in CHS ;* May 1993

NIFS-228 Y. Ohkouchi, S. Sasaki, S. Takamura, T. Kato, *Effective Emission and Ionization Rate Coefficients of Atomic Carbons in Plasmas;* June 1993

NIFS-229 K. Itoh, M. Yagi, A. Fukuyama, S.-I. Itoh and M. Azumi, *Comment on 'A Mean Field Ohm's Law for Collisionless Plasmas;* June 1993

NIFS-230 H. Idei, K. Ida, H. Sanuki, H. Yamada, H. Iguchi, S. Kubo, R. Akiyama, H. Arimoto, M. Fujiwara, M. Hosokawa, K. Matsuoka, S. Morita, K. Nishimura, K. Ohkubo, S. Okamura, S. Sakakibara, C. Takahashi, Y. Takita, K. Tsumori and I. Yamada, *Transition of Radial Electric Field by Electron Cyclotron Heating in Stellarator Plasmas;* June 1993

NIFS-231 H.J. Gardner and K. Ichiguchi, *Free-Boundary Equilibrium Studies for the Large Helical Device,* June 1993

NIFS-232 K. Itoh, S.-I. Itoh, A. Fukuyama, H. Sanuki and M. Yagi, *Confinement Improvement in H-Mode-Like Plasmas in Helical Systems,* June 1993

NIFS-233 R. Horiuchi and T. Sato, *Collisionless Driven Magnetic Reconnection,* June 1993

NIFS-234 K. Itoh, S.-I. Itoh, A. Fukuyama, M. Yagi and M. *Azumi, Prandtl Number of Toroidal Plasmas;* June 1993